ELSEVIER

Earth and Planetary Science Letters 206 (2003) 571–585

EPSL

www.elsevier.com/locate/epsl

Magnetic hysteresis monitoring of Cretaceous submarine basaltic glass during Thellier paleointensity experiments: evidence for alteration and attendant low field bias

Alexei V. Smirnov, John A. Tarduno *

Department of Earth and Environmental Sciences, University of Rochester, Rochester, NY 14627, USA

Received 4 October 2002; received in revised form 22 November 2002; accepted 23 November 2002

Abstract

On the basis of studies of Holocene samples, submarine basaltic glass (SBG) is thought to be an ideal paleointensity recorder because it contains unaltered single domain magnetic inclusions that yield Thellier paleointensity data of exceptional quality. To be useful as a recorder of the long-term geomagnetic field, older SBG must retain these optimal properties. Here, we examine this issue through rock magnetic and transmission electron microscope (TEM) analyses of Cretaceous SBG recovered at Ocean Drilling Program Site 1203 (northwestern Pacific Ocean). These SBG samples have very low natural remanent magnetization intensities (NRM < 50 nAm^2/g) and TEM analyses indicate a correspondingly low concentration of crystalline inclusions. Thellier experiments on samples with the strongest NRM intensity ($> 5\times10^{-11}$ Am^2) show a rapid acquisition of thermoremanent magnetization (TRM) with respect to NRM demagnetization. Taken at face value, this behavior implies magnetization in a very weak (< 17 μT) ambient field. But monitoring of magnetic hysteresis properties during the Thellier experiments (on subsamples of the SBG samples used for paleointensity determinations) indicates systematic variations in values over the same temperature range where the rapid TRM acquisition is observed. A similar change in properties during heating is observed on monitor SBG specimens using low-temperature data: with progressive heatings the Verwey transition becomes more distinct. We suggest that these experimental data record the partial melting and neocrystallization of magnetic grains in SBG during the thermal treatments required by the Thellier method, resulting in paleointensity values biased to low values. We further propose that this process is pronounced in Cretaceous and Jurassic SBG (relative to Holocene SBG) because devitrification on geologic time scales (i.e., tens of millions of years) lowers the transition temperature at which the neocrystallization can commence. Magnetic hysteresis monitoring may provide a straightforward means of detecting the formation of new magnetic inclusions in SBG during Thellier experiments.

Keywords: submarine basaltic glass; magnetic hysteresis; paleointensity; transmission electron microscopy; devitrification

1. Introduction

A long-term paleointensity record is essential for a complete description of the geomagnetic

* Corresponding author. Tel.: +1-716-275-5713; Fax: +1-716-244-5689.
E-mail address: john@earth.rochester.edu (J.A. Tarduno).

0012-821X/02/$ – see front matter © 2002 Elsevier Science B.V. All rights reserved.
doi:10.1016/S0012-821X(02)01123-8

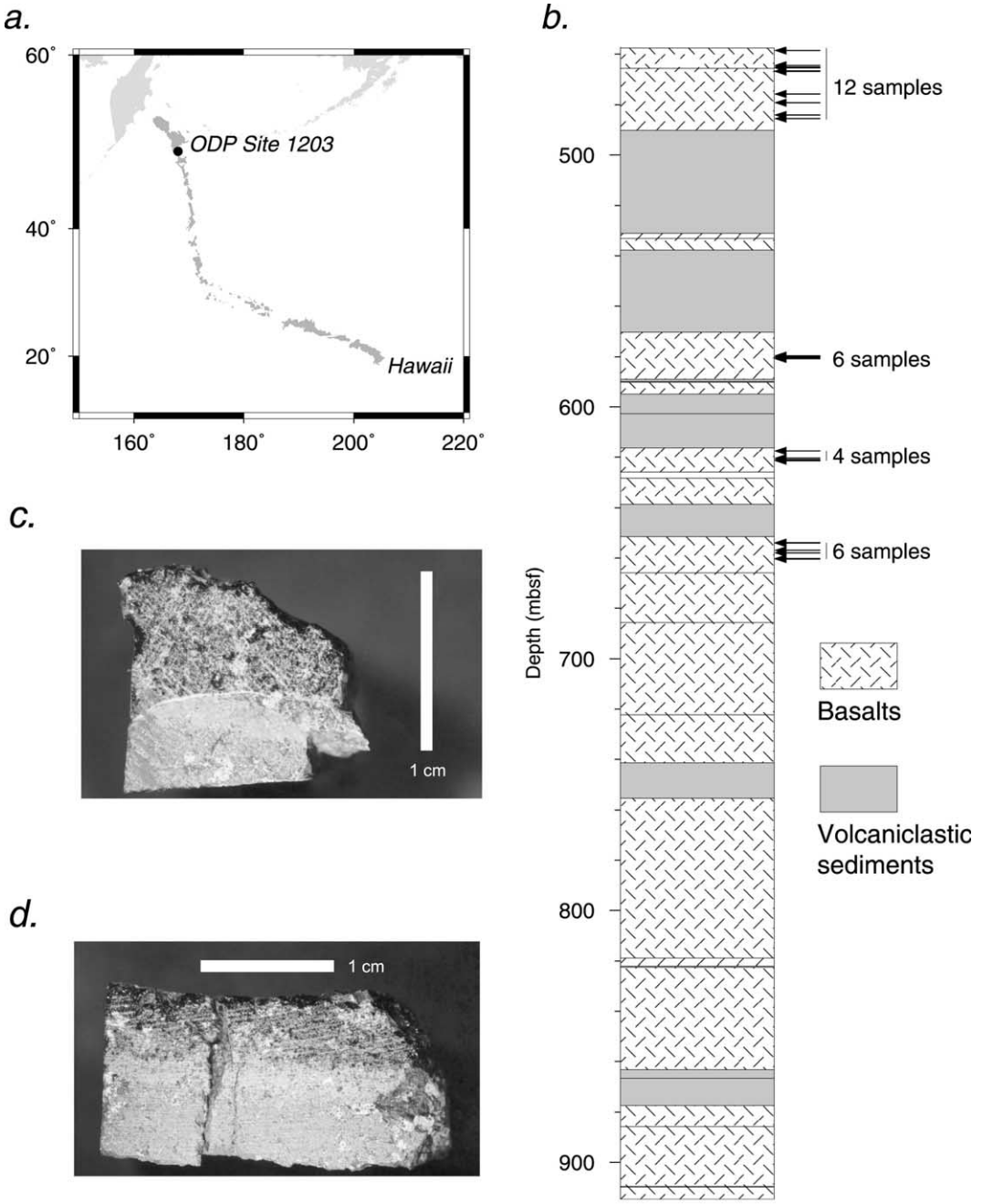

Fig. 1. (a) Location of ODP Leg 197 Site 1203 (Detroit Seamount). (b) Simplified stratigraphy of basalt section from ODP Site 1203. Lava flows are shown by stippled pattern, volcaniclastics are shown by gray color. Depths of sampling (meters below sea floor, mbsf) are shown by arrows. (c,d) Typical ODP Site 1203 samples with glassy margins.

field, as well as for gaining an understanding of the long-term magnetic signature of oceanic crust. However, in contrast to the detailed information available on the directional behavior of the field (e.g., [1–4]), data constraining the past intensity of the geomagnetic field remain scarce. More than one third of paleointensity data cover only the last 5 Myr [5]. Fewer rocks from older epochs are available for study because of weathering and metamorphism; these factors can corrupt primary paleointensity signals. The Thellier–Thellier technique [6], arguably the most reliable method of paleointensity determination, often fails on whole rock samples because of mineralogical alteration during the successive heating steps required by the method. This problem has motivated a search for alternative paleointensity recorders [7,8].

Based on their study of Holocene samples from the East Pacific Rise, Pick and Tauxe [7] suggested that submarine basaltic glass (SBG) might be an ideal paleointensity recorder. High unblocking temperatures of natural remanent magnetization (NRM) (>400°C), Curie temperatures between 490 and 550°C, and saturation of isothermal remanent magnetization (IRM) at 0.2–0.3 T indicated that low-Ti magnetite was the carrier of magnetic remanence [7]. Holocene SBG also showed wasp-waisted magnetic hysteresis loops which were interpreted as recording a mixture of single domain (SD) and superparamagnetic (SP) grains. The presence of grains close in size to the SP/SD threshold was consistent with the high magnetic viscosity reported for Holocene SBG [7]: a viscous remanent magnetization acquired in a 0.9 mT field decayed within 1 h.

Little alteration of the Holocene SBG was detected during Thellier-type laboratory heating, but the formation of magnetite was reported after heating to 600°C during thermomagnetic analysis [7]. The latter type of alteration was likened to the decomposition of titanomaghemite into ilmenite and low-Ti magnetite [7,9]. The success of paleointensity experiments using SBG is supported by results from recent lava flows [10,11] which have yielded the known geomagnetic field intensity at the site [7,12]. This promise is somewhat dampened by the results of Carlut and Kent [11] who report paleointensity values from recent SBG of the Juan de Fuca Ridge which were only within $\pm 30\%$ of the known geomagnetic intensity. However, this low apparent accuracy might be related to large magnetic anomalies at the sampling site [11].

Magnetic characteristics of Cretaceous SBG samples were reported to be similar to those of Holocene SBG [12,13], although the former seem to have slightly higher NRM unblocking (>500°C) and Curie temperatures (565–575°C). Observations using transmission electron microscopy (TEM) show the presence of 10–20 nm (presumably, magnetite) inclusions in the Cretaceous SBG [13]. However, while room temperature magnetic susceptibilities after subsequent heatings of Holocene SBG remained constant (up to 550°C), those measured from some Cretaceous glasses showed a noticeable increase after heating above 400°C [13]. Regardless of this difference, Cretaceous SBG also appears to have yielded nearly ideal paleointensity data [14]. Interestingly, for ages older than 0.5 Ma, SBG has yielded relatively low paleointensities (e.g., [5,14]). If correct, these data suggest that the last 0.5 million years is a special period characterized by an unusually high intensity of the geomagnetic field.

Recent drilling of the Emperor Seamounts during Ocean Drilling Program (ODP) Leg 197 resulted in the recovery of SBG, providing another opportunity to constrain the past intensity of the Earth's magnetic field. In this paper we report results of rock magnetic and TEM analyses of these glasses in order to assess their suitability for paleointensity study, and to investigate the more general question of whether older SBG retains the optimal properties reported for Holocene samples.

2. Submarine basaltic glass from ODP Site 1203

Drilling at ODP Site 1203 (Fig. 1a) at Detroit Seamount of the Emperor Seamounts (northwestern Pacific Ocean) resulted in the recovery of 18 lava units and 14 volcaniclastic interbeds in 453 m of basement penetration [15]. The sequence is approximately 76 Myr old [15]. Twenty-eight SBG

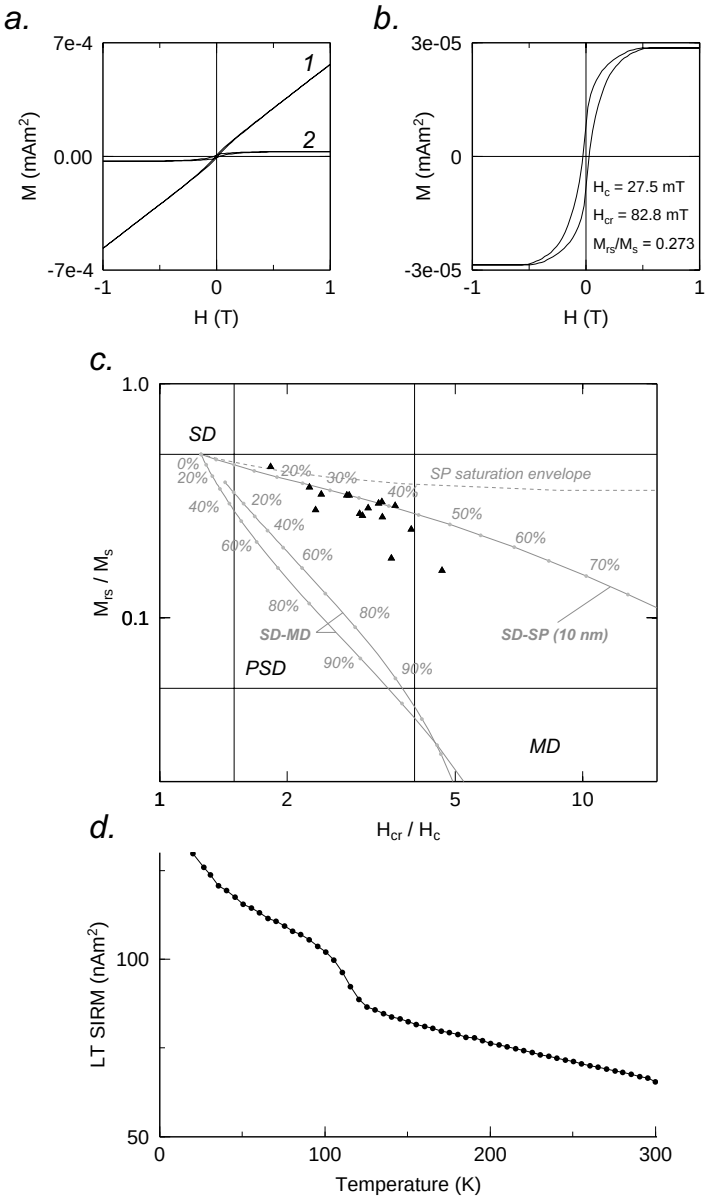

Fig. 2. (a) Typical magnetic hysteresis loop for SBG (ODP Site 1203) before (1) and after (2) paramagnetic slope correction as measured on an AGFM. (b) Typical magnetic hysteresis loop after paramagnetic slope correction. Slightly wasp-waisted loops were observed for some samples. (c) Magnetic hysteresis ratios plotted on Day diagram [16]. Abbreviations are: SD, single domain; PSD, pseudo-single domain; MD, multidomain; SP, superparamagnetic). Only data points for which the signal/noise ratio (defined as the ratio between the total M_s and the M_s of the AGFM P1-type probe) is larger than five are shown. Gray lines are theoretical curves for mixtures of MD and SD grains (MD–SD lines, based on two different datasets), and SP (10 nm in size) and SD grains (SD–SP line) after [17]. Numbers along curves are volume fractions of SP or MD component in mixtures with SD grains. Dashed gray line shows SP saturation envelope, when H_c is large enough so that the Langevin function saturates [17]. (d) Thermal demagnetization curve of low-temperature saturation isothermal remanent magnetization (LT SIRM) imparted in a glass sample at 20 K.

samples from five of the lava units were selected for shore-based analysis (Fig. 1b).

Our samples are small 1–2 cm thick pieces of rock with glassy margins (Fig. 1c,d). The glass margin is usually thin (1–2 mm), but in several samples it reaches ~5 mm. The SBG appears to be unaltered (with the exception of the lowermost sample from 660.32 m below sea floor, mbsf), but often shows significant surficial oxidation. Areas of unaltered glass are surrounded by more oxidized fractures within the overall glass margin. The unaltered glass could be separated easily along these fractures.

Nearly equant subsamples of SBG ~1.5–2 mm in size were cleaned using an ultrasound treatment in 1.7 N hydrochloric acid (~15 min) followed by rinsing in isopropanol and distilled water. All rock magnetic, TEM and paleointensity experiments were conducted on these clean glass fragments.

Table 1
Magnetic hysteresis parameters for samples from ODP Site 1203

Depth mbsf	H_c mT	H_{cr} mT	M_{rs}/M_s
458.45	33.6	94.3	0.334
464.41	34.0	94.0	0.334
465.00	28.6	103.0	0.301
465.07	29.8	99.9	0.313
465.32	27.5	82.8	0.273
465.40	22.9	75.4	0.308
466.70	29.5	91.8	0.295
466.75	27.7	109.0	0.239
475.68	15.3	54.0	0.180
479.19	24.6	73.1	0.279
579.61	35.0	81.7	0.289
580.17	31.4	75.7	0.337
580.52	17.4	80.9	0.159
621.06	47.0	106.0	0.362
621.06	59.6	109.0	0.442
621.46	26.7	89.7	0.270

The signal/noise ratio (defined as the ratio of the total M_s to the M_s of the AGFM P1-type probe) is larger than five for all data points.

3. Rock magnetic and TEM analyses

3.1. Rock magnetic analyses

Magnetic hysteresis parameters (coercivity H_c, coercivity of remanence H_{cr}, saturation remanence M_{rs}, and magnetization of saturation M_s) and the acquisition of IRM were measured using a Princeton Measurements Corporation alternating gradient force magnetometer (AGFM) at the University of Rochester. Although the AGFM is highly sensitive and we employed only P1-type sample probes, magnetic hysteresis measurements of the SBG proved to be very difficult due to their low magnetizations. In fact, paramagnetism is dominant (the paramagnetic component was up to 98% of the M_s) (Fig. 2a). Three SBG samples showed completely paramagnetic behavior.

Magnetic hysteresis parameters for the samples with a clear ferromagnetic component after paramagnetic slope correction (Fig. 2b, Table 1) plot in the pseudo-single domain (PSD) region of the Day diagram [16] (Fig. 2c). More recently the Day plot has been refined by Dunlop [17]; the otherwise huge PSD field has been divided into regions reflecting mixtures of SD and multidomain grains and SD and SP grains. Our samples appear to be more consistent with the latter type of mixture. Values which plot below the SD–SP trend (Fig. 2c) may reflect viscous SD particles with magnetic properties dominated by thermal activation [18]. Some of the magnetic hysteresis loops are slightly wasp-waisted (Fig. 2b), further supporting the presence of SP grains. IRM acquisition curves saturate at ~0.2–0.4 T. No significant changes of magnetic hysteresis parameters or IRM acquisition behavior were observed with depth.

Low-temperature magnetic characteristics of the SBG were determined using a Quantum Design magnetic property measurement system (MPMS) at the Institute of Rock Magnetism (University of Minnesota). Glass chips were first fixed into gelatin capsules using a non-magnetic fiberglass filling. The capsule was then tightly packed in a plastic straw (which is a standard sample holder for the MPMS). Each sample was first cooled to 20 K in a zero magnetic field environment. Then a SIRM was imparted by applying a 2.5 T magnetic field for 60 s. Next the superconducting magnet was immediately quenched

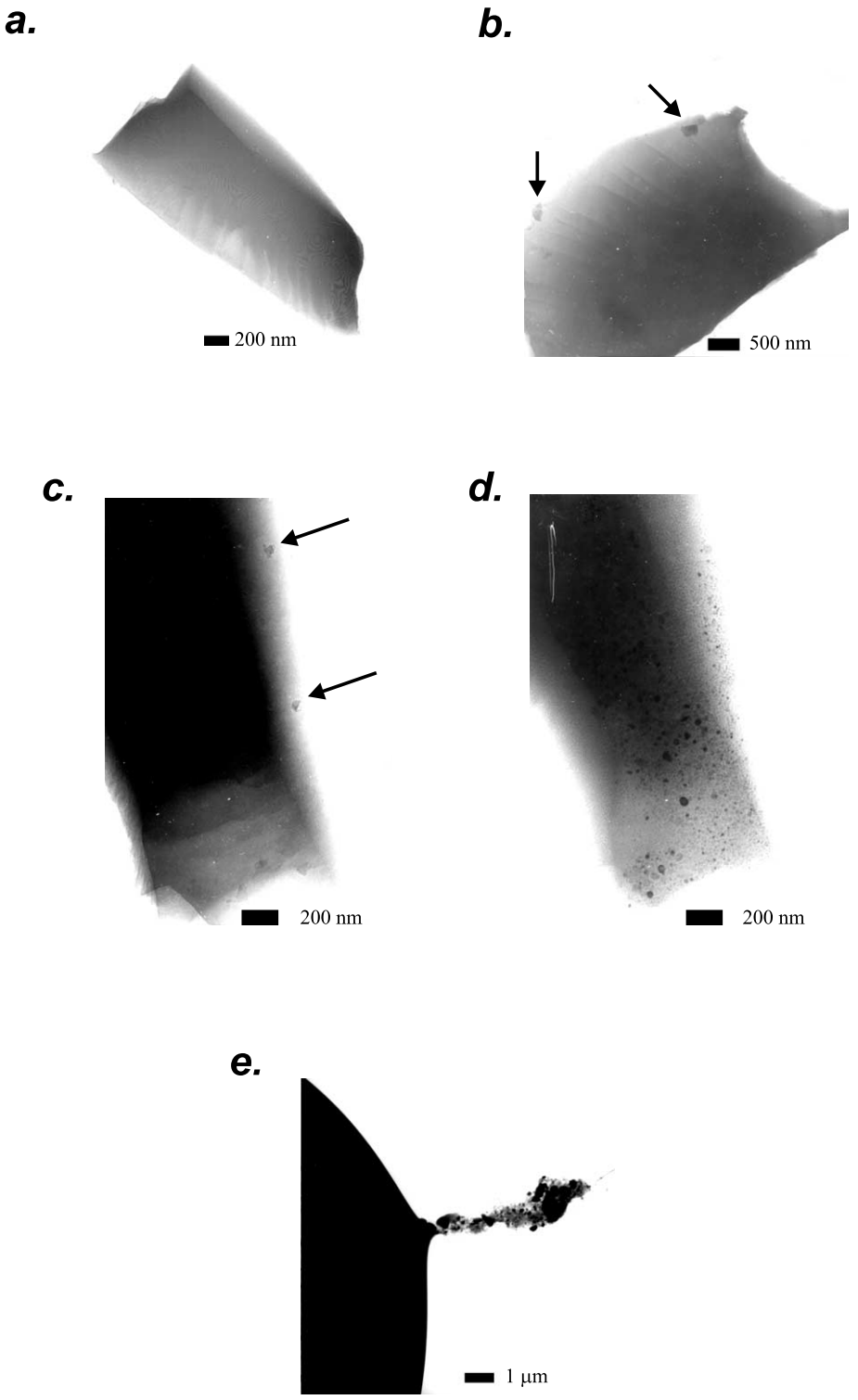
a.
200 nm
b.
500 nm
c.
200 nm
d.
200 nm
e.
1 μm

(reset) using an ultralow field coil to reduce the residual field to <1 μT (as measured by a fluxgate magnetometer; M. Jackson, personal communication, 2002). Thermal demagnetization of the LT SIRM was measured during zero field warming to room temperature (300 K) at 5 K steps. A slightly blurred Verwey transition was observed within the range 110–120 K for all samples (Fig. 2d). The manifestation of the Verwey transition in the SIRM data at such temperatures indicates the presence of relatively well-preserved magnetite particles. The 'blurring' suggests either oxidation, or the presence of Ti in the lattice.

3.2. TEM analyses

Several clean SBG chips were crushed into a fine assemblage of shards (using a sapphire mortar and pestle) to be used in TEM analyses. The fine shards were deposited on carbon films mounted on copper grids. The analyses were performed using a JOEL JEM 2000 Ex, 200 keV microscope at the University of Rochester.

In most cases, the SBG shards appeared to contain no inclusions (Fig. 3a). This observation is consistent with recent reports that large number of glasses must be tested in order to identify samples with NRMs strong enough for paleointensity measurement. For example, in studies of Neogene SBG, some 90% of the samples have been excluded because of their low NRM intensities [19]. In some shards a few nearly equant crystalline inclusions (as shown by dark field imaging [20]) 20–100 nm in size were observed (Fig. 3b). Overall, our TEM experiments were hampered by the rapid melting of glass fragments due to heating by absorption of the electron beam. This melting occurred only after a few minutes of exposure under the electron beam. Nevertheless, thinner fragments, transparent to electrons, could be used for TEM analysis.

Sometimes changes were observed in the SBG shards immediately prior to complete melting. While the shape of a sample remained approximately constant, the leaf-like texture characteristic of fresh glass disappeared and was replaced by a 'sugary' texture (Fig. 3d); we suggest this may reflect partial melting of the glass. In all cases this process also resulted in the appearance of multiple inclusions. The crystalline nature of these new inclusions was confirmed by dark field imaging. The inclusions, which were 10–80 nm in size, may have formed from crystallization of Fe ions in the glass. Continued heating under the electron beam eventually resulted in the complete melting of such samples. Sometimes aggregates of crystalline particles were ejected from the melted glass (Fig. 3e).

4. Paleointensity experiments and monitoring of magnetic hysteresis properties

4.1. Experimental procedure

Only subsamples of SBG with magnetic moment greater than 5×10^{-11} Am^2 (5×10^{-8} emu) were selected for paleointensity experiments. About 90% of subsamples measured (five to seven subsamples from each of 28 ODP samples) were rejected because of their weak magnetic moments. Sixteen SBG samples were studied using the stepwise double heating Thellier method as modified by Coe [21]. Each sample was attached to a 3 mm diameter (Pyrex) quartz tube using a non-magnetic, high-temperature cement. The quartz tubes were placed in a brass sample holder for heating in an ASC TD-48 thermal demagnetization device. Magnetic remanence of the samples was measured using a 2G DC superconducting quantum interference device (SQUID) magnetometer (with a 4 cm access and a high-resolution coil

←

Fig. 3. TEM analyses of SBG (ODP Site 1203). (a) Glass containing no visible inclusions. (b) Glass with two inclusions shown by arrows. (c) TEM image of a glass sample (ODP Site 1203) before melting. Two inclusions are shown by arrows. (d) The same sample after partial melting. Multiple crystalline inclusions are seen. (e) Glass after complete melting by the electron beam. Material ejected from the melted glass contains crystalline aggregates.

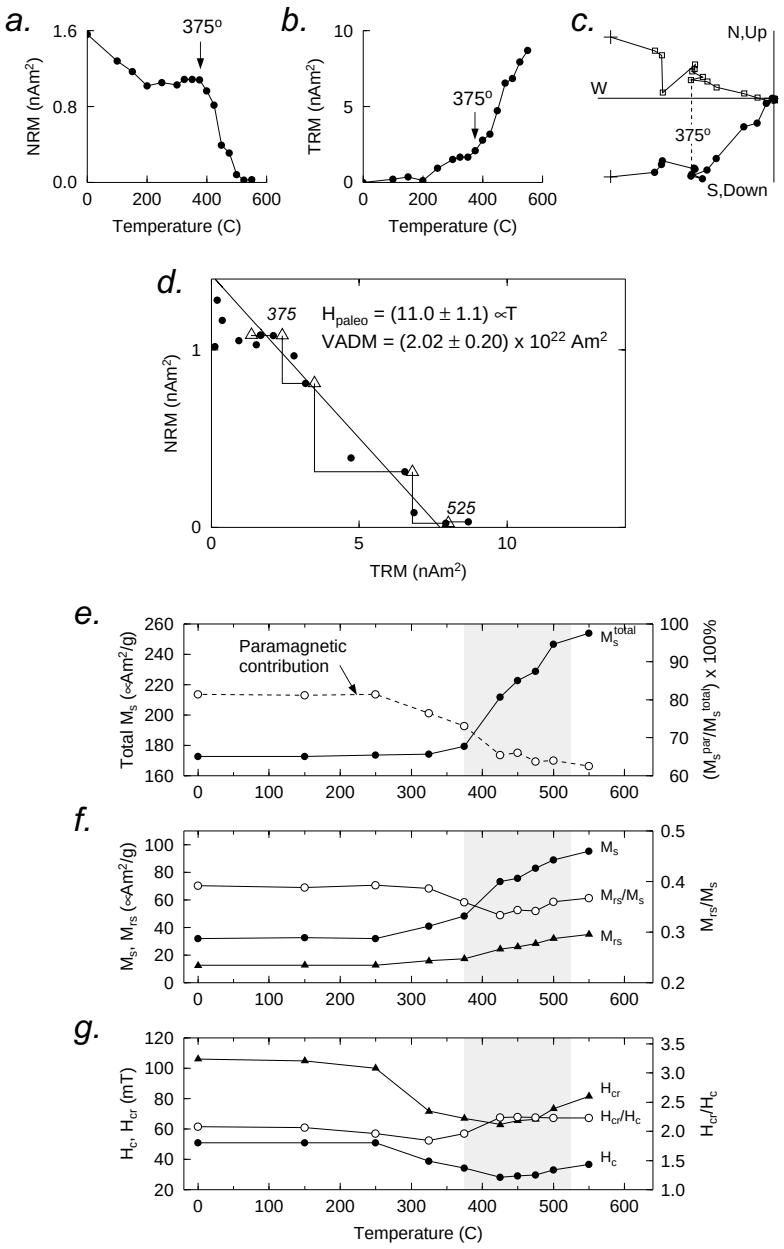

Fig. 4. (a–d) Paleointensity determination from SBG of ODP Site 1203 (621.06 mbsf). (a) Thermal demagnetization of the NRM. (b) pTRM acquisition. (c) Orthogonal vector plot of field-off steps for the unoriented sample (vertical projection of NRM, open squares; horizontal projection of NRM, closed circles). (d) NRM–TRM plot (circles). Triangles are pTRM checks. (e–g) Magnetic hysteresis parameters as a function of heating temperature on a split of the SBG sample from 621.06 mbsf. (e) The total saturation magnetization (M_s^{total}) before slope correction (solid circles, solid line). Paramagnetic contribution: The difference (M_s^{par}) between the M_s^{total} and the saturation magnetization (M_s) after slope correction normalized to the M_s^{total} (open circles, dashed line). (f) Saturation magnetization (M_s) after slope correction (solid circles), saturation remanent magnetization (M_{rs}) (solid triangles), and the M_{rs}/M_s ratio (open circles). (g) Coercivity (H_c, solid circles), coercivity of remanence (H_{cr}, solid triangles), and the H_{cr}/H_c ratio (open circles). Gray boxes show the temperature range used to calculate the paleointensity value.

geometry) at the University of Rochester. A laboratory field of 60 μT was used. Samples were heated and cooled in air for 45 min. Due to the very fast natural cooling rates (T. Thordarsson, personal communication, 2002), no cooling rate correction was needed [22,23].

A temperature increment of 25°C was used. To monitor possible alteration during the experiment, partial thermoremanent magnetization (pTRM) checks were utilized for temperatures >250°C: after every second off-field temperature step, an on-field step at a lower temperature was measured. To be judged successful a pTRM check must fall within 5% of the original TRM value. The other reliability criteria for paleointensity determination used are described elsewhere (e.g., [8]).

In addition to paleointensity measurements, duplicate specimens (splits) of six of the glass samples were prepared to study magnetic hysteresis parameters as a function of temperature (T_h). These splits were placed in ceramic non-magnetic boats and heated together with samples used for paleointensity determinations. Hence, they should provide good monitors of the behavior of the samples used for paleointensity determination [24]. After cooling, hysteresis parameters of the duplicate samples were measured at room temperature using the AGFM. In addition to recording M_s, M_{rs}, H_c, and H_{cr}, we used the total saturation magnetization (M_s^{tot}) before slope correction and M_s to estimate the paramagnetic signal. Before and after the experiment all split samples were weighed using a Mettler Toledo AG 245 Balance at the University of Rochester.

4.2. Paleointensity results

Three SBG samples with the weakest NRM intensity showed erratic directional behavior during the Thellier experiment (probably due to the low signal/noise ratios) and are not considered further here. The remaining samples showed regular directional demagnetization behavior with one high-temperature component (~375–525°C) (Figs. 4 and 5). However, 50% of the samples failed to pass pTRM checks (the deviation of the pTRM check from the initial pTRM value was within ±20%). Interestingly, a rapid increase of pTRM occurs at approximately the same temperature interval as the definition of the high-temperature component (Fig. 4b). Because of this rapid increase, the total TRM was 3–20 times that of the NRM.

Only five samples met paleointensity reliability criteria; these yielded relatively low paleointensity values (Table 2). For example, Thellier results shown in Figs. 4 and 5 suggest paleointensities of 11 ± 1 μT and 9 ± 1 μT, respectively. The corresponding values of virtual dipole moment (VDM) are $2.0 \pm 0.2 \times 10^{22}$ Am^2 and $1.6 \pm 0.1 \times 10^{22}$ Am^2 (using a paleolatitude of 35° [15]).

4.3. Magnetic hysteresis monitoring results

Surprisingly, magnetic hysteresis parameters of the SBG monitor 'split' samples showed a systematic pattern with heating. No significant changes were observed until T_h of ~325–400°C (e.g., Figs. 4e–g and 5e–g). Heating to higher temperatures resulted in a significant increase of M_s^{tot} (110–150%), M_s (140–300%), M_{rs} (140–280%). These changes coincided with a decrease in the paramagnetic component of the total magnetization signal (100–250%). For all samples studied the temperature at which these changes occur approximately corresponded to the temperature of the onset of the rapid increase of pTRM (Figs. 4 and 5) which would otherwise be used to constrain paleointensity. Coercivity values also showed systematic patterns in the same temperature interval.

Table 2
Nominal paleointensity values from SBG of ODP Site 1203 passing standard reliability criteria

Depth mbsf	F μT	VDM 10^{22} Am^2
458.45	11.2 ± 2.0	2.06 ± 0.37
465.00	9.0 ± 0.8	1.65 ± 0.15
479.19	17.3 ± 2.2	3.18 ± 0.40
485.47	8.8 ± 0.6	1.62 ± 0.11
621.06	11.0 ± 1.1	2.02 ± 0.20

F is field intensity. Virtual dipole moment (VDM) is calculated based on a paleolatitude of 35° [15]. Uncertainties are 1σ.

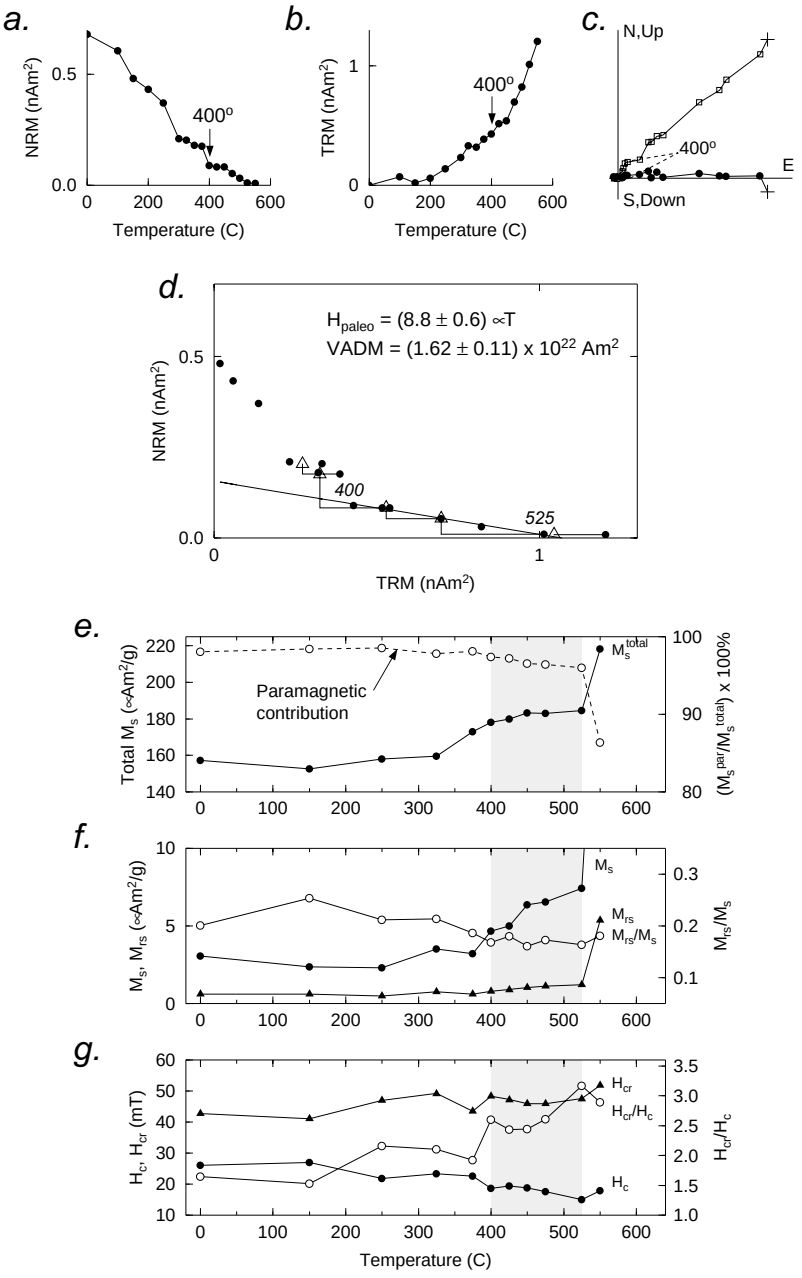

Fig. 5. (a–d) Paleointensity determination from SBG of ODP Site 1203 (485.47 mbsf). (a) Thermal demagnetization of the NRM. (b) pTRM acquisition. (c) Orthogonal vector plot of field-off steps for the unoriented sample (vertical projection of NRM, open squares; horizontal projection of NRM, closed circles). (d) NRM–TRM plot (circles). Triangles are pTRM checks. (e–g) Magnetic hysteresis parameters as a function of heating temperature on a split of the SBG sample from 485.47 mbsf. (e) The total saturation magnetization (M_s^{total}) before slope correction (solid circles, solid line). Paramagnetic contribution: The difference (M_s^{par}) between the M_s^{total} and the saturation magnetization (M_s) after slope correction normalized to the M_s^{total} (open circles, dashed line). (f) Saturation magnetization (M_s) after slope correction (solid circles), saturation remanent magnetization (M_{rs}) (solid triangles), and the M_{rs}/M_s ratio (open circles). (g) Coercivity (H_c, solid circles), coercivity of remanence (H_{cr}, solid triangles), and the H_{cr}/H_c ratio (open circles). Gray boxes show the temperature range used to calculate the paleointensity value.

4.4. Monitoring using demagnetization of LT SIRM

To investigate the cause of the increases of M_s and M_{rs} discussed above we attempted another type of monitoring experiment using the demagnetization of LT SIRM. The experimental procedure for the SIRM measurement was as described previously. However, after a complete SIRM demagnetization experiment was performed on an unheated SBG sample, we subsequently heated the same sample to 250°C in a NEY 2-525 oven (in air) for ~4 h at the Institute of Rock Magnetism. We then repeated the SIRM demagnetization experiment. Next, the sample was heated to 450°C (~4 h) and the SIRM demagnetization experiment was performed. While no change in low-temperature magnetic behavior was observed after heating to 250°C, the treatment at 450°C resulted in an increased LT SIRM and a much sharper Verwey transition (Fig. 6). Together, these changes indicate the formation of magnetite.

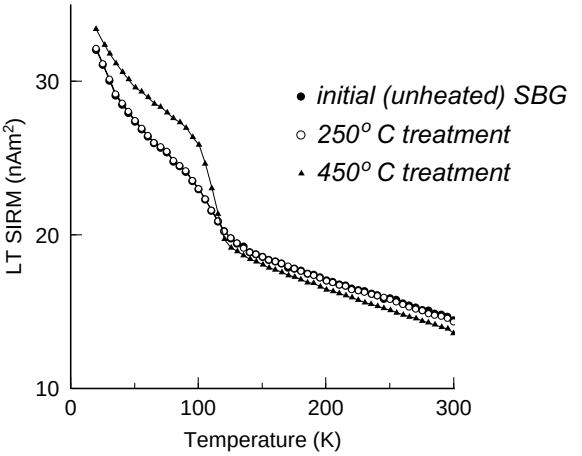

Fig. 6. Thermal demagnetization curves of LT SIRM measured on an ODP Site 1203 glass sample before (solid circles) and after heating to 250°C (open circles) and 450°C (solid triangles). The initially blurred Verwey transition becomes sharper after heating to 450°C.

5. Discussion

At first glance, the paleointensity data from the ODP Site 1203 SBG samples that meet standard reliability criteria (Table 2) seem to confirm the low VDM values reported from other Cretaceous SBGs (e.g., [14]). However, our results of the magnetic hysteresis monitoring during the Thellier runs indicate that a new magnetic material forms in our glasses upon heating. Because this process coincides with a rapid increase of pTRM acquisition (at temperatures >350–400°C), the attendant low paleointensity values are suspect. Monitoring using demagnetization of LT SIRM indicates that the new magnetic mineral formed is magnetite.

One possible mechanism for the creation of magnetite is the alteration of clay minerals, similar to that proposed by Cottrell and Tarduno [8] to explain paleointensity properties of some bulk volcanic rocks. Little or no alteration is suggested by our TEM analyses, which showed that the glass shards retained a leaf-like texture characteristic of fresh glass (e.g., Fig. 3a,b). Nevertheless, it is possible that clays are present in the larger samples used for the Thellier analysis.

Another mechanism, which we note for the first time here and feel may be the predominant cause of the observed rock magnetic changes, is hinted at by the melting of SBG we observed during TEM analyses. Namely, the SBG may undergo partial melting during the Thellier experiments resulting in the neocrystallization of small magnetite particles from iron ions. This mechanism is supported by the simultaneous increase of M_{rs} and M_s, and the decrease of the paramagnetic component as iron ions (which contribute to the paramagnetic component) are consumed during the formation of new magnetite crystals.

Glasses are thermodynamically unstable and with time and/or under a variety of conditions may become crystalline. At room temperature this process is very slow, but it may accelerate at elevated temperatures within the transitional range (e.g., [25]) and result in the appearance of crystalline inclusions similar to those we observed during partial melting. For example, Schlinger et al. [26] observed the formation of SP magnetite in glass from tuff after heating to 730–980°C.

In contrast to crystalline solids, glasses do not have distinct melting points. When a glass is

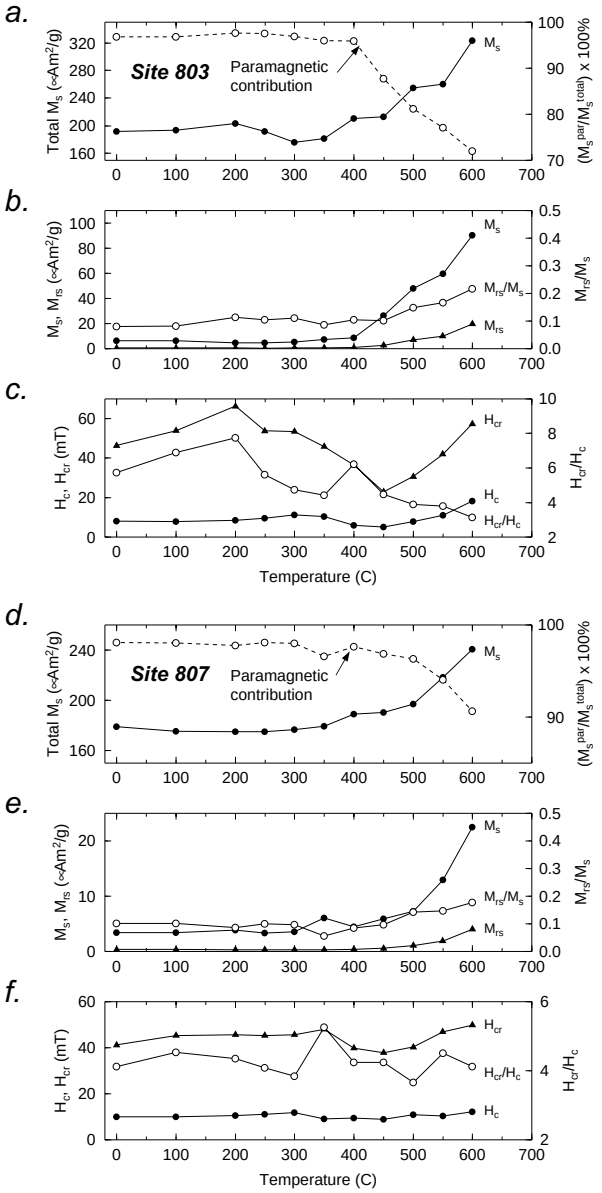

Fig. 7. (a–c) Magnetic hysteresis parameters as a function of heating temperature for a SBG sample from ODP Site 803. (a) The total saturation magnetization (M_s) before paramagnetic slope correction (solid circles, solid line). Paramagnetic contribution: The difference (M_s^{par}) between the M_s^{total} and the saturation magnetization (M_s) after slope correction normalized to the M_s^{total} (open circles, dashed line). (b) Saturation magnetization (M_s) after slope correction (solid circles), saturation remanent magnetization (M_{rs}) (solid triangles), and the M_{rs}/M_s ratio (open circles). (c) Coercivity (H_c, solid circles), coercivity of remanence (H_{cr}, solid triangles), and the H_{cr}/H_c ratio (open circles). (d–f) Magnetic hysteresis parameters as a function of heating temperature for a SBG sample from ODP Site 807. (d) The total saturation magnetization (M_s) before paramagnetic slope correction (solid circles, solid line). Paramagnetic contribution: The difference (M_s^{par}) between the M_s^{total} and the saturation magnetization (M_s) after slope correction normalized to the M_s^{total} (open circles, dashed line). (e) Saturation magnetization (M_s) after slope correction (solid circles), saturation remanent magnetization (M_{rs}) (solid triangles), and the M_{rs}/M_s ratio (open circles). (f) Coercivity (H_c, solid circles), coercivity of remanence (H_{cr}, solid triangles), and the H_{cr}/H_c ratio (open circles).

heated, the chemical bonds holding the atoms break over a range of temperatures (the so-called transformation range). As a result, a glass softens (melts) gradually as it heats. This process is usually quantified by the glass transition temperature (T_g), which is approximately the mid-point of the transformation range [27,28]. The database on the transition temperatures of natural volcanic glass is limited, but available estimates suggest that its T_g may be as low as 400–450°C (e.g., [27,29]). Synthetic glass may have T_g as low as 400°C (Schott catalog Optical Glass 10022e). Such synthetic glasses are melted during TEM experiments similar to those we performed (B. McIntyre, personal communication). Therefore, the partial melting under the TEM we observed may have been caused by temperatures as low as 400°C. Given such a low temperature, partial melting may also occur during Thellier experiments.

Enhanced diffusion of iron ions associated with heating under the electron beam (prior to partial melting) might also contribute to the formation of crystalline inclusions in SBG. The relative importance of this mechanism, however, depends on the rates of diffusion of iron. Because of its relatively small ionic radius (e.g., 0.83 Å for Fe^{2+} [30]) iron is known as a fast diffuser (e.g., [31,32]). In crystalline silicon at 500°C iron is characterized by a relatively rapid diffusion coefficient of $\sim 10^{-7}$ cm^2/s (e.g., [31,33]). However, diffusion rates in silicon are generally many orders of magnitude greater than those in glass. Unfortunately, direct measurements of diffusion coefficients for iron in basaltic glass are not available. But we can get some idea of the diffusion rate by assuming that Fe^{2+} will behave similarly to other divalent ions. For example, calcium has a diffusion coefficient between 10^{-14} and 10^{-15} cm^2/s at 500°C in a soda-lime silicate glass [34]. If Fe behaves similarly, it is unlikely that diffusion prior to partial melting can solely account for the formation of new crystalline inclusions in SBG.

The simultaneous increase of M_{rs} and decrease of a paramagnetic signal (implied by the increase in ferromagnetic contribution, Figs. 4e and 5e) we observed indicate that the size of some of these newly formed magnetic grains should be larger than the SP/SD threshold. We suggest that heating of SBG during paleointensity experiments can form an ensemble of ferromagnetic grains characterized by a broad grain size distribution. Such a model is consistent with changes in H_c and H_{cr} in some samples which may record the variable concentration of SP particles in the total population of new grains (and/or changes in the internal structure of grains as they grow) (Fig. 4).

To test whether the glass samples we have studied are representative of SBG in general, we measured the dependence of room temperature magnetic hysteresis properties upon heating for samples of Cretaceous SBG from ODP Sites 803 and 807 ($\sim$90 and $\sim$122 Ma, respectively) from Ontong Java Plateau [35] that have been used previously in Thellier paleointensity experiments [12,14]. All samples showed magnetic behavior similar to that observed for SBG samples from ODP Site 1203 (Fig. 7). In particular, we observed an increase of the M_s and M_{rs} accompanied by a decrease in the paramagnetic contribution to the total magnetization at temperatures $>$400°C. These observations suggest that the neocrystallization of magnetic grains upon heating may be a common feature of Cretaceous SBG. It may be responsible for the increase in the room temperature magnetic susceptibility after heating to 450–500°C reported by Pick and Tauxe [13].

At this point we should address the apparent difference in magnetic behavior between Holocene and older SBG. Indeed, while modern SBG appears to be resistant to alteration during Thellier experiments, Cretaceous SBG, as we have shown, may alter upon heating. We suggest that age is a dominant factor determining at what temperature, and to what extent, the thermally induced neocrystallization occurs. We hypothesize that older SBG may be more susceptible to experimental alteration because the chemical bonds in glass can soften over tens of millions of years resulting in a lowered transition temperature (and, hence, the temperature at which the partial melting and the formation of new crystalline inclusions may occur). This process may be especially significant in submarine environments where hydration may further decrease the transition temperature and accelerate the process of devitrification (e.g., [25,27,36]).

Thus, we suggest that the paleointensity measured from Cretaceous SBG of ODP Site 1203 (and probably some Cretaceous SBG from other sites) is biased to lower values due to the formation of new ferromagnetic grains during paleointensity experiments. This mechanism may contribute to some very low paleointensity values reported from SBG older than 0.5 Ma (e.g., [5]).

Another important observation is that in some cases this process does not result in a violation of any standard reliability criteria, including pTRM checks (Figs. 4 and 5). One reason for this may be that the neocrystallization is a gradual process which occurs over a wide range of temperatures so that its cumulative effect may not be seen by pTRM checks done at small (e.g., 25–50°C) temperature steps. Therefore, the application of these traditional criteria may not be sufficient to detect the appearance of a new ferromagnetic phase in some volcanic glasses.

One variable that we have not fully explored in our study is heating time. For our Thellier experiments we use a heating time of 45 min. Some prior studies of SBG use a comparable time [10] while others adopt a shorter heating time at the maximum temperature of a given Thellier step [7]. In many studies, however, the heating time is not specified and the cumulative effect of heating is hard to gauge.

The relationship between SBG age, devitrification and response to Thellier thermal treatment, however, is likely to be complex. It is therefore unlikely that neocrystallization can be excluded solely by employing short heating times. To address this uncertainty we propose that the monitoring of magnetic hysteresis properties be used to identify potential partial melting and neocrystallization. Such measurements should be added to the list of standard reliability criteria when using SBG for paleointensity determinations.

6. Conclusions

Rock magnetic and TEM analyses performed on SBG from ODP Site 1203 (Detroit Seamount) show that, in spite of their relatively good preservation, they are unlikely to retain reliable paleointensity information. Over a temperature that yields paleointensity data that pass standard reliability criteria, we observe systematic changes in magnetic hysteresis properties signaling the formation of new magnetic particles. We interpret these data as a record of the partial melting of the glass in the course of Thellier heatings. The newly formed magnetic particles result in paleointensity values which are artificially low.

We hypothesize that the partial melting and precipitation of new magnetic inclusions may be common in SBG of the Cretaceous age as a result of their lowered transition temperatures caused by devitrification. On the other hand, Holocene glass may have transition temperatures higher than those normally used for Thellier experiments so that neocrystallization is minor. This may explain (at least in part) consistently lower paleointensities reported from SBG older than 0.5 Ma.

Our results suggest that great care should be taken to gauge alteration when using pre-Holocene SBG for paleointensity analyses. In particular, we propose that, in order to detect the partial melting and neocrystallization processes, magnetic hysteresis parameters should be monitored.

Acknowledgements

We thank Brian McIntyre for help with TEM analyses, Paul Funkenbusch and Robert Doremus for useful discussions, Don Peacor, Andrei Kosterov, and Yongjae Yu for helpful reviews, and the Institute for Rock Magnetism (University of Minnesota) for a Visiting Fellowship (to A.S.). Funds for the Institute for Rock Magnetism are provided by the Keck Foundation and the University of Minnesota. This research used samples provided by the Ocean Drilling Program (ODP). ODP is sponsored by the U.S. National Science Foundation (NSF) and participating countries under management of Joint Oceanographic Institutions (JOI), Inc. Funding for this research was provided by JOI/USSSP and the National Science Foundation (Geophysics Program).*[RV]*

References

[1] E. Irving, Paleomagnetism and its Application to Geological and Geophysical Problems, Wiley, New York, 1964, 399 pp.

[2] R. Van der Voo, Paleomagnetism of the Atlantic, Tethys and Iapetus Oceans, Cambridge University Press, Cambridge, 1993, 411 pp.

[3] R.T. Merrill, M.W. McElhinny, P.L. McFadden, The Magnetic Field of the Earth: Paleomagnetism, the Core and the Deep Mantle, Academic Press, San Diego, CA, 1996, 531 pp.

[4] M.W. McElhinny, P.L. McFadden, Paleomagnetism: Continents and Oceans, Academic Press, San Diego, CA, 2000, 386 pp.

[5] M.T. Juarez, L. Tauxe, J.S. Gee, T. Pick, The intensity of the Earth's magnetic field over the past 160 million years, Nature 394 (1998) 878–881.

[6] E. Thellier, O. Thellier, Sur l'intensité du champ magnétique terrestre dans le passé historique et géologique, Ann. Geophys. 15 (1959) 285–376.

[7] T. Pick, L. Tauxe, Holocene paleointensities: Thellier experiments on submarine basaltic glass from the East Pacific Rise, J. Geophys. Res. 98 (1993) 17949–17964.

[8] R.D. Cottrell, J.A. Tarduno, Geomagnetic paleointensity derived from single plagioclase crystals, Earth Planet. Sci. Lett. 169 (1999) 1–5.

[9] R.S. Coe, S. Gromme, E.A. Mankinen, Geomagnetic paleointensities from radiocarbon dates lava flows on Hawaii and the question of the Pacific non-dipole low, J. Geophys. Res. 83 (1978) 1059–1069.

[10] V. Mejia, N.D. Opdyke, M.R. Perfit, Paleomagnetic field intensity recorded in submarine basaltic glass from the East Pacific Rise, the last 69 Ka, Geophys. Res. Lett. 23 (1996) 475–478.

[11] J. Carlut, D.V. Kent, Paleointensity record in zero-age submarine basalt glasses: Testing a new dating technique for recent MORBs, Earth Planet. Sci. Lett. 183 (2000) 389–401.

[12] T. Pick, L. Tauxe, Geomagnetic palaeointensities during the Cretaceous normal superchron measured using submarine basaltic glass, Nature 366 (1993) 238–242.

[13] T. Pick, L. Tauxe, Characteristics of magnetite in submarine basaltic glass, Geophys. J. Int. 119 (1994) 116–128.

[14] P.A. Selkin, L. Tauxe, Long-term variations in palaeointensity, Phil. Trans. R. Soc. 358 (2000) 1065–1088.

[15] J.A. Tarduno, R.A. Duncan, D.W. Scholl et al., Proc. ODP Leg Init. Reports 197 (2002) 92 pp.

[16] R. Day, M. Fuller, V.A. Schmidt, Hysteresis properties of titanomagnetites: Grain-size and compositional dependence, Phys. Earth Planet. Inter. 13 (1977) 260–267.

[17] D.J. Dunlop, Theory and application of the Day plot (M_{rs}/M_s versus H_{cr}/H_c) 1. Theoretical curves and tests using titanomagnetite data, J. Geophys. Res. 107 (2002) 10.1029/2001JB000486.

[18] L. Lanci, D.V. Kent, Introduction to thermal activation in forward modeling of SD hysteresis loops and implications for the interpretation of the Day diagram, Quad. Geofis. 26 (2002) 91–92.

[19] M.T. Juarez, L. Tauxe, The intensity of the time-averaged geomagnetic field: the last 5 Myr, Earth Planet. Sci. Lett. 175 (2000) 169–180.

[20] G. Meek, Practical Electron Microscopy for Biologists, Wiley, New York, 1976, 528 pp.

[21] R.S. Coe, Paleointensities of Earth's magnetic field determined from Tertiary and Quaternary rocks, J. Geophys. Res. 72 (1967) 3247–3262.

[22] S.E. Halgedahl, R. Day, M. Fuller, The effect of cooling rate on the intensity of weak-field TRM in single-domain magnetite, J. Geophys. Res. 85 (1980) 3690–3698.

[23] E. McClelland Brown, Experiments on TRM intensity dependence on cooling rate, Geophys. Res. Lett. 11 (1984) 205–208.

[24] M. Haag, J.R. Dunn, M. Fuller, A new quality check for absolute palaeointensities of the Earth magnetic field, Geophys. Res. Lett. 22 (1995) 3549–3552.

[25] R.R. Marshall, Devitrification of natural glass, Geol. Soc. Am. Bull. 72 (1961) 1493–1520.

[26] C.M. Schlinger, D. Griscom, G.C. Papaefthymiou, D.R. Veblen, The nature of magnetic single domains in volcanic glasses of the KBS tuff, J. Geophys. Res. 93 (1988) 9137–9156.

[27] V. Bouska, Natural Glasses, Ellis Horwood, New York, 1993, 354 pp.

[28] E.-J. Donth, The Glass Transition: Relaxation Dynamics in Liquids and Disordered Materials, Springer, New York, 2001, 418 pp.

[29] S. Sakka, J.D. MacKenzie, Relation between apparent glass transition temperature and liquidus temperature for inorganic glasses, J. Non-Cryst. Sol. 6 (1971) 145–162.

[30] D.J. Dunlop, Ö. Özdemir, Rock Magnetism: Fundamentals and Frontiers, Cambridge University Press, Cambridge, 1997, 573 pp.

[31] W. Frank, U. Gösele, H. Mehrer, A. Seeger, Diffusion in silicon and germanium, in: G.E. Murch, A.S. Nowick (Eds.), Diffusion in Crystalline Solids, Academic Press, Orlando, FL, 1984, pp. 63–142.

[32] R.H. Doremus, Diffusion of Reactive Molecules in Solids and Melts, Wiley, New York, 2002, 293 pp.

[33] A.A. Istratov, H. Hieslmair, E.R. Weber, Iron and its complexes in silicon, Appl. Phys. A 69 (1999) 13–44.

[34] N.P. Bansal, R.H. Doremus, Handbook of Glass Properties, Academic Press, Orlando, FL, 1986, 680 pp.

[35] J.A. Tarduno, W.V. Sliter, L. Kroenke, M. Leckie, H. Mayer, J.J. Mahoney, R. Musgrave, M. Storey, E.L. Winterer, Rapid formation of Ontong Java plateau by Aptian mantle plume volcanism, Science 254 (1991) 399–403.

[36] R. Doremus, Glass Science, Wiley, New York, 1994, 339 pp.